ELSEVIER

Journal of Fluids and Structures 21 (2005) 731–742

JOURNAL OF FLUIDS AND STRUCTURES

www.elsevier.com/locate/jfs

Nonlinear airship aeroelasticity

N. Bessert[1], O. Frederich*,[2]

Flight Science, CargoLifter Development GmbH, Germany

Received 4 January 2005; accepted 15 September 2005
Available online 18 October 2005

Abstract

The aeroelastic derivatives for today's aircraft are calculated in the concept phase using a standard procedure. This scheme has to be extended for large airships, due to various nonlinearities in structural and aerodynamic behaviour. In general, the structural model of an airship is physically as well as geometrically nonlinear. The main sources of nonlinearity are large deformations and the nonlinear material behaviour of membranes. The aerodynamic solution is also included in the nonlinear problem, because the deformed airship influences the surrounding flow. Due to these nonlinearities, the aeroelastic problem for airships can only be solved by an iterative procedure. As one possibility, the coupled aerodynamic and structural dynamic problem was handled using linked standard solvers. On the structural side, the Finite-Element program package ABAQUS was extended with an interface to the aerodynamic solver VSAERO. VSAERO is based on the aerodynamic panel method using potential flow theory. The equilibrium of the internal structural and the external aerodynamic forces leads to the structural response and a trimmed flight state for the specified flight conditions (e.g. speed, altitude). The application of small perturbations around a trimmed state produces reaction forces and moments. These constraint forces are then transferred into translational and rotational acceleration fields by performing an inertia relief analysis of the disturbed structural model. The change between the trimmed flight state and the disturbed one yields the respective aeroelastic derivatives. By including the calculated derivatives in the linearised equation of motion system, it is possible to judge the stability and controllability of the investigated airship.

Keywords: Airship; Aeroelasticity; ABAQUS; VSAERO; Panel method; Inertia relief

1. Introduction

As for most vehicles, the question of stability and controllability is also to be answered for airships, with the only exception that the answer is known in advance: airships do not fly stable! But is the magnitude of instability acceptable? Is the pilot still able to control the airship?

At the beginning of the 20th century aeroelastic effects were observed for the Siemens–Schuckert airship (Haas and Dietzius, 1913). While flying out of control over a lake, the shadow of the airship revealed the cause of the controllability problem. The airship was deformed like a banana due to sideforces on the vertical tail planes. For those

*Corresponding author. Tel.: +49 30 314 24415; fax: +49 30 314 25405.
E-mail address: octavian.frederich@cfd.tu-berlin.de (O. Frederich).
[1]Altair Engineering GmbH, Böblingen, Germany.
[2]Hermann-Föttinger-Institute of Fluid Mechanics, Berlin University of Technology, Germany.

0889-9746/$ - see front matter
doi:10.1016/j.jfluidstructs.2005.09.005

large airships of the era, the controllability requirements such as limiting speed, the size of fins and of control surfaces, were determined empirically with the one-to-one models. Today such requirements have to be known before the first flight. With the current technology in structural and aerodynamic simulation, aeroelastic effects can be predicted. To quantify them, the change in aerodynamic loads due to small perturbations from an equilibrium state must be determined. Therefore, the assumption of static and steady-state conditions is sensible.

To investigate the influence of aerodynamics on the structural behaviour of the airship, in general an adjusted structural and aerodynamic description for the airship is required. In addition, the controllability of flight-mechanical degrees of freedom must be provided in both models. The interaction between the aerodynamics and the structure can be realised by a coupling algorithm.

The effort of providing and coupling different models for the various fields can be reduced if there is a base model from which all other are directly derived. For this base model a parametric structural model for the airship was used. Originally, this model (Section 2) was developed to analyse the assembly procedure and response to any specified load case. It must therefore be enhanced for use in the aeroelastic investigations (Section 3).

The basis of the aeroelastic investigations conducted is the equation of motion system for the centre of mass of an airship. These governing equations are the same for all structures:

$$\mathbf{m}\cdot\ddot{\mathbf{x}}=\mathbf{F}\quad\text{and}\quad\boldsymbol{\theta}\cdot\ddot{\boldsymbol{\phi}}=\mathbf{M},\tag{1.1}$$

where $\mathbf{m}$ and $\boldsymbol{\theta}$ are the mass and inertial properties including aerodynamic masses and $\ddot{\mathbf{x}}$ and $\ddot{\boldsymbol{\phi}}$ denote the translational and rotational degrees of freedom. The external forces $\mathbf{F}$ and moments $\mathbf{M}$ can be subdivided according to their corresponding physical causes. Besides resultant forces due to aerostatics and gravity, there is also a dependence on the aerodynamics of the actual deformed shape and the thruster forces. Additionally, all accelerations vanish for the trimmed flight state, so one obtains

$$\begin{aligned}&\mathbf{F}_{\text{aerodyn}}+\mathbf{F}_{\text{aerostat}}+\mathbf{F}_{\text{thrust}}+\mathbf{F}_{\text{grav}}=\mathbf{0},\\&\mathbf{M}_{\text{aerodyn}}+\mathbf{M}_{\text{aerostat}}+\mathbf{M}_{\text{thrust}}+\mathbf{M}_{\text{grav}}=\mathbf{0}.\end{aligned}\tag{1.2}$$

If this equilibrium state is disturbed, the external forces can be linearised with the aeroelastic derivatives for the stability analysis. The coupling scheme and the obtained results are shown in Section 4 together with a discussion of the physical influences, before a conclusion is given.

2. Structural model

The global structural behaviour of the investigated airship CL160 was analysed using the finite element method. In order to manage different configurations, a parametric model was generated using MSC.Patran (2001). The parameterisation incorporated some trivial geometric properties, e.g. airship shape (length and slenderness), the number of nose battens, the size of fins, number of cables, keel position, number of engines, etc., as well as the finite element discretisation and parameters, e.g. number of elements, their mechanical properties (mass, stiffness, material model) can be adapted. In addition, there are some special details like integration of fin control surfaces, keel hinge and ballonets adaptable. The aim of this parametrically defined whole airship model was the prediction of the structural deformation and the interface loads for the detail constructors. On the one hand, all predefined load cases could be calculated by changing global configuration parameters such as mass, ballonet state, pressure, etc. On the other, sensitivity and parameter studies could be performed by the adaption of local structural properties, e.g. stiffness, pretension, etc.

The geometry of the airship is based on the so-called Gertler shape, a measured and parameterised drag-minimised airship hull. This base body of revolution and all further structural parts of the airship were discretized by finite elements. Therefore, many different element types had to be used. The envelope, nose and tail which are subjected to internal and aerostatic pressure were defined as membrane or shell elements, respectively, whereas the fins were modelled as continua and their bracing cables as truss elements. For each part of the airship a respective finite element was chosen and provided with elaborate properties. The internal gas was modelled by distributing its mass to the elements forming the envelope, and the internal pressure was applied to each of these elements. In addition, the aerostatic pressure was defined in the structural model with a pressure gradient and a reference height derived from the altitude.

In Fig. 1, two variants of the complete airship mesh are shown. Apart from the different refinement level of the meshing, it can be recognised that the keel model is reduced to the structurally relevant parts. In contrast to all covering patterns which have no influence on the structural behaviour and therefore did not have to be modelled, the relevant masses such as payload and engines were considered as concentrated at their centres of mass. Fig. 2 gives an overview of

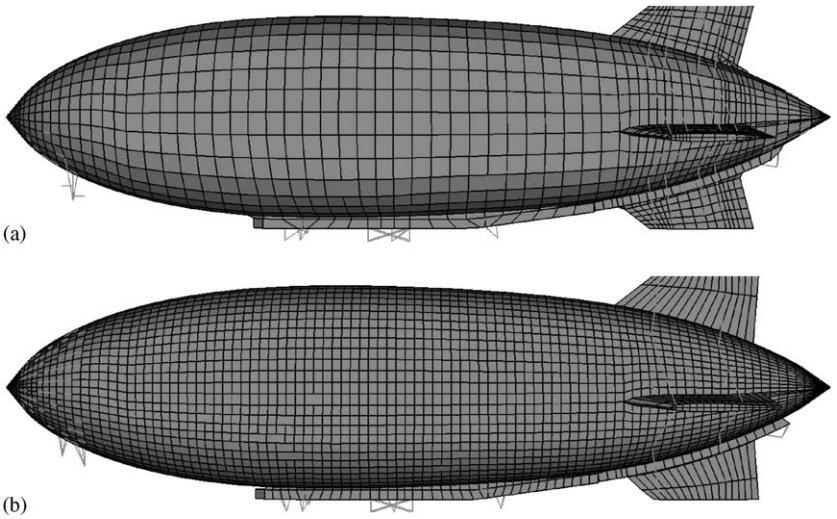

Fig. 1. Structural airship models with different parameterisation: (a) coarse grid with aerodynamic adaptions; (b) normal grid for loadcase calculations.

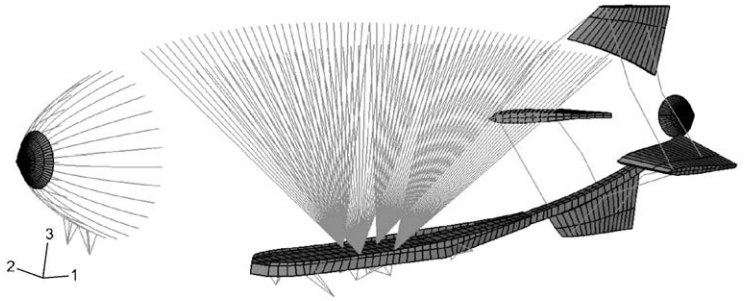

Fig. 2. Keel, suspension, nose battens and empennage with bracing cables.

the parts arranged around the airship envelope, with the ballonets removed for clarity. The number of suspension cables, nose battens and bracing cables could easily be changed in the parametric model, as could their properties. Besides, the complete model could also be extended to include further parameterisation and properties.

The structural behaviour of the whole airship model was predicted using the finite element package ABAQUS (Hibbitt et al., 2001). This solver was chosen because it is capable of handling all occurring structural nonlinearities including large deformation, membrane elements with nonlinear orthotropic material and the wrinkling model. In addition, it allows the inclusion of user-defined models to be implemented through subroutines. For example, the special material properties of the airship hull were defined in this way. To simulate the assembly procedure of the airship, ABAQUS provides the possibility of arranging elements with and without strain, another source of nonlinearity. In ABAQUS the structural problem is integrated in an updated Lagrangian formulation, and the resulting general nonlinear structural equation system is solved using the Newton–Raphson method (Zienkiewicz and Taylor, 1991) with linesearch-backtracking. The implicit solver used is highly developed, and by adaptive control of the iterative solving algorithm, the convergence could be improved. The convergence criterion is based on flux and force formulation, whereby the size of the load increments is adjusted with respect to previous convergence behaviour.

For each different model configuration defined with the parametric model, the assembly of the airship had to be simulated. The stepwise assembly procedure was appropriately modelled following the different actions that were planned for the real-life airship assembly. The simulated work steps were: (i) pressurisation of the envelope, (ii) strain-free addition of the keel and nose battens, (iii) addition of the suspension cables with strain and application of buoyancy and gravity, (iv) strain-free addition of fins, (v) application of tension on the bracing cables and (vi) restraint under out-of-hangar boundary conditions and application of correct pressure gradient. The finally assembled airship in the

so-called out-of-hangar state is already deformed compared to the reference geometry, and was used as the starting point for the loadcase calculations or the aeroelastic investigations.

3. Integration of aerodynamics

For the aerodynamic solver, the commercial VSAERO was used. This panel code requires the complete aerodynamic surface to be described as patches and panels. The surface panels were directly created from the structural finite elements, thereby eliminating the need for interpolation between two different mesh distributions. Each three or four nodes of a finite element corresponded to a four-node linear-bordered panel. This connection was the basic idea behind the coupling of structural mechanics and aerodynamics, however there were some requirements to fulfill beforehand. The following paragraphs describe modifications to the basic structural model (used for load case calculations) in order to define an aerodynamic closed surface and to include required control parameters.

Because at first only the choice of physical and numerical influence parameters should be investigated, a relatively coarse structural grid was used, as previously shown in Fig. 1(a). The use of a model with real aerodynamic grids on all surfaces is too complex for practicable aeroelastic investigations. The increase in accuracy for a very high number of panels and elements was found to be very small compared to the increase in computing time. This is even more the case when it is considered that ABAQUS and VSAERO exchange the geometric and aerodynamic solutions with each other in an iterative manner.

The aerodynamic surface was defined in the structural model as three- or four-noded membranes or shell elements. These must be grouped into different patches building a quadrangle, where triangles as degenerated variants are allowed. It was ensured that all element normals pointed towards the outside of the airship surface.

For structural investigations the influence of some parts of the airship could be neglected, especially the covering patterns. The resulting gaps in the structural model had to be closed for the aerodynamic grid. The elements for closing such gaps were allocated a very low stiffness (a hundredth of the other membranes) so that they did not influence the structure.

In the structural model the fins were modelled as solids with elaborate properties. The complete fin model was adapted for deriving and controlling an aerodynamic model. First, the surface of the solid fins were covered with equivalent weak surface elements. To achieve a better aerodynamic solution on the fin surface, the grid lines were compressed in the direction of the leading edge (bias meshing). In a second step, the moveable control surfaces were integrated. For this, a part of each fin was extracted from the structure and linked to the fin with connectors and an actuator (Fig. 3). The control surfaces could be moved via the actuators by heating the actuator material (of thermal expansion coefficient 1.0). The required temperature difference for a specified rudder angle was calculated from the geometrical connection between the activator and the control surface.

The gaps at the control surfaces were again covered by membrane elements with low stiffness. These elements were added strain-free after the rudder was deflected, whereas the deflection had to be carried out before the coupled analysis. Another aspect to be considered before the analysis was the necessity of sharp trailing edges for the attachment of wake lines. The panel code in VSAERO delivers zero drag unless wake lines leaving the trailing edges of the fins are defined, which model the wake. All the wake lines, including the stitched wake line (Fig. 4), were discretized using wake grid planes.

In VSAERO, a panel code based on potential flow theory is used to obtain the aerodynamic solution. VSAERO is able to calculate the nonlinear aerodynamic characteristics of arbitrary configurations solving the Neumann problem of potential flow. Nonlinear effects of wake shape are treated in an iterative wake relaxation procedure. The vorticity shed into the flow by the passage of the body is represented by the wake in VSAERO. The wake is described by a set of wake lines aligned approximately with the local flow, whereby the points describing each wake line lie in wake grid planes

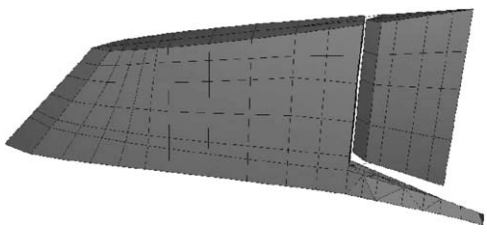

Fig. 3. Fin with moveable control surface.

common to all the wakes simplifying the relaxation of the wake. The wake is aligned with local streamlines in an iterative process (Nathman, 1999). The influence of the aerodynamics can be controlled with the pitch angle α, the slip angle β, and with Reynolds number Re (if the boundary layer effect is to be taken into account). The elevator angle η and the rudder angle ζ were controlled by the moveable control surfaces of the structural model. In addition to the control parameters, the flight conditions are given in general by the velocity V, the density ρ and the altitude H (already included in the structural model).

4. Fluid–structure interaction

4.1. Coupling scheme

The aim of the coupling of ABAQUS and VSAERO was the determination of an equilibrium between the aerodynamic forces (steady) and the structural dynamic forces of an elastic structure (see Fig. 5). In terms of

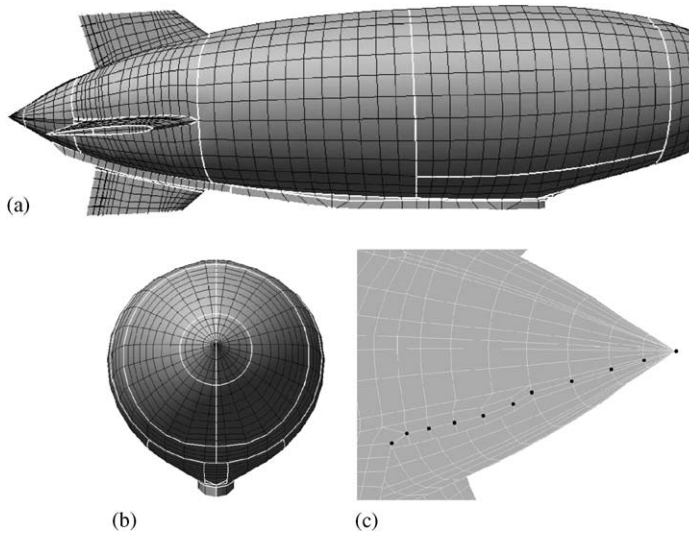

Fig. 4. Aerodynamic model with patches and panels in VSAERO: (a) side view; (b) front view; (c) stitched wake line.

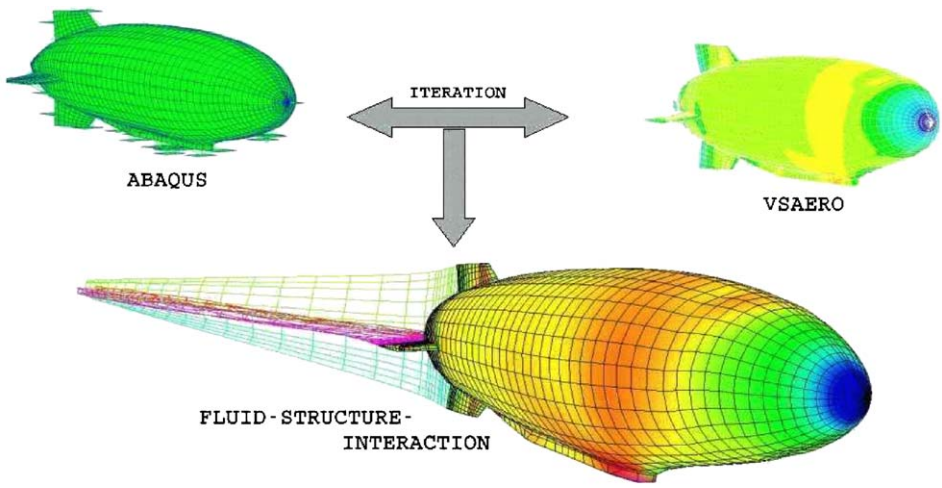

Fig. 5. Fluid–structure interaction.

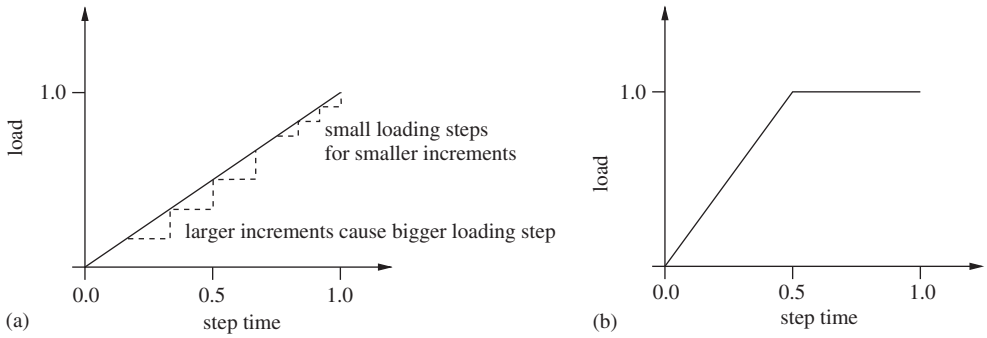

Fig. 6. Load ramping over one step using ABAQUS: (a) standard; (b) adapted.

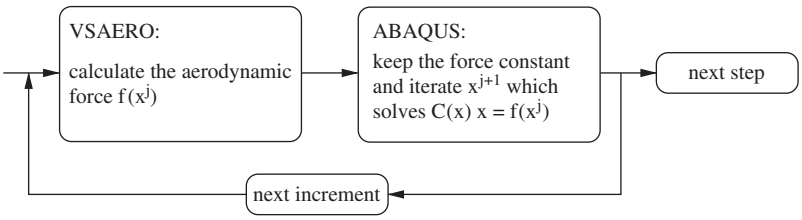

Fig. 7. Iteration scheme.

mathematics, this fixed-point problem can be written as

$$\underbrace{\mathbf{C}(\mathbf{x}).\mathbf{x}}_{\text{struct. force}} - \underbrace{\mathbf{f}(\mathbf{x})}_{\text{aerodyn. force}} = \mathbf{0}, \tag{4.1}$$

where $\mathbf{C}(\mathbf{x})$ is the structural stiffness. This nonlinear equation can be solved iteratively by

$$\mathbf{x}^{i+1} = \mathbf{C}^{-1}(\mathbf{x}^i) \cdot \mathbf{f}(\mathbf{x}^i). \tag{4.2}$$

For arbitrary external loads $\mathbf{f}(\mathbf{x})$, Eq. (4.2) can be solved using a standard ABAQUS calculation. Because of various nonlinearities, e.g. material behaviour and large deformations, the solution can be obtained only by an iterative algorithm (Newton–Raphson). Usually a step is divided into several increments and the load is not applied at once, but increased linearly over the step to ensure and accelerate convergence to an equilibrium for a constant load (Fig. 6(a)).

ABAQUS provides subroutines for the application of user-defined element pressures and to manage external databases. The structural elements defining the aerodynamic surface were sorted by such a user subroutine into the format VSAERO requires for the panel definitions (Nathman, 1999). This geometric (aerodynamic) model was sent to VSAERO in each increment to obtain an aerodynamic solution. Using the current aerodynamic forces as a constant external load, Eq. (4.2) was solved in all increments for the coupled problem (Fig. 7).

Keeping the aerodynamic force constant during the structural deflection of the airship required some increments for relaxation after the full aerodynamic load (proportional to the dynamic pressure) had been applied. Therefore the standard load application scheme of ABAQUS was adapted in the way that the magnitude of the load was increased linearly over the first half of the step. In the second half, the fully applied dynamic pressure was held constant and an equilibrium between external aerodynamic load and internal structural forces could be achieved (Fig. 6(b)).

The load curve shown in Fig. 6(b) is divided, as is usual in ABAQUS, into discrete load increments, that separate the step equidistantly for this case. The number of increments per step also determines the number of iterative interchanges between the solvers. Therefore, it had to be demonstrated that the chosen increment size did not influence the results. The increment sizes of 0.1, 0.05 and 0.025 were tested. The quality of the numerical solution can be judged by the rate of change of the force during the iteration. The global force can be expressed by the lift coefficient of the aerodynamic model or by the reaction forces of the structural dynamic model. A converged solution is obtained if the forces, which are directly correlated to the deformation of the airship, have a horizontal tangent. In Fig. 8 it can be seen that an

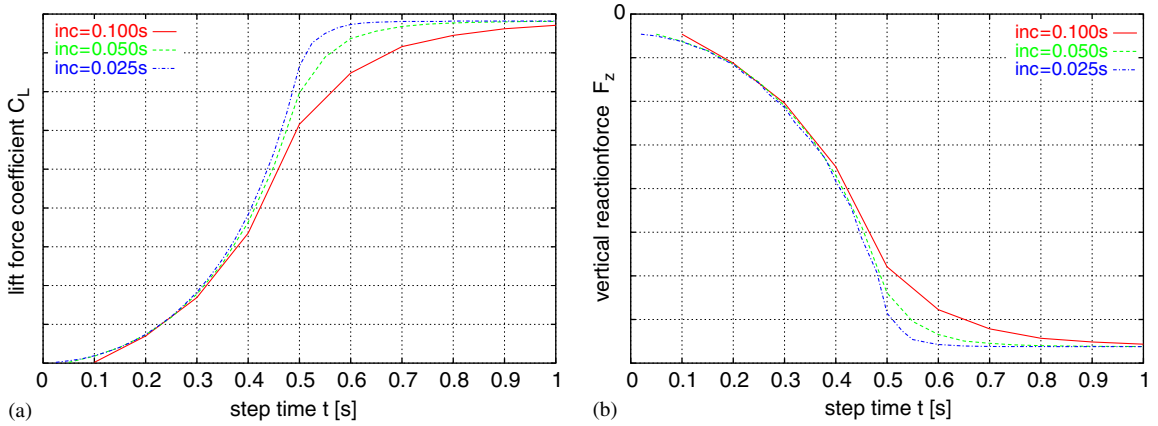

Fig. 8. Forces over one step depending on the increment size. (a) Aerodynamic lift force; (b) structural reaction force.

increment size of 0.05 was found to be small enough to achieve this criterion. This increment size is used for all further investigations.

The deformed airship from the previous structural increment became the new shape evaluated in the aerodynamic calculation. For each airship shape a new pressure distribution c_p was calculated for all panels. These pressures were introduced into the structural model as element loads with the dynamic pressure $\frac{1}{2}\rho V^2$ to $p = c_p q$. The pressure was applied to each element by the aeroelastic coupling procedure in the positive element-normal direction. Through visualisation of the pressures via a user-defined variable in ABAQUS, the correct application could be verified.

4.2. Trimmed flight state

The starting point for all the aeroelastic investigations was the trimmed air-ship. Naturally this trimmed flight is already a result of interaction between structural and aerodynamic behaviour and represents the static equilibrium for straight and level flight. This had to be obtained via the aeroelastic coupling procedure for ABAQUS and VSAERO, for which Eq. (4.3) was solved with respect to the flight trim parameters: α—pitch angle, η—elevator angle, and $\mathbf{F}_{\text{thrust}}$—thrust force (Fig. 9):

$$\begin{aligned}&\mathbf{F}_{\text{aerodyn}} + \mathbf{F}_{\text{aerostat}} + \mathbf{F}_{\text{thrust}} + \mathbf{F}_{\text{grav}} = \mathbf{0},\\ &\mathbf{M}_{\text{aerodyn}} + \mathbf{M}_{\text{aerostat}} + \mathbf{M}_{\text{thrust}} + \mathbf{M}_{\text{grav}} = \mathbf{0}.\end{aligned} \tag{4.3}$$

The rigid body motion of the structural model was restrained by the kinematic coupling of three very stiff nodes at the loadframe (Fig. 10). In an equilibrium state these additional reaction forces must become zero.

Besides the coupled nonlinear aerodynamic and structural models, the determination of the equilibrium state due to various parameters is another nonlinear problem. This was formulated as minimisation, where the goal function (Eq. (4.4)) was given by the length of the vector of all reaction forces and moments. To obtain an even-conditioned equation system, the moments were additionally normalised by the length of the airship. The resulting multidimensional minimisation problem was solved with a Lines-Search iteration scheme from Numerical Recipes (Press et al., 1996). Each iteration was a fully coupled aeroelastic calculation with modified flight trim parameters,

$$\begin{pmatrix}\mathbf{RF}(\alpha,\eta,F_{\text{thrust}})\\ \mathbf{RM}(\alpha,\eta,F_{\text{thrust}})/l_{\text{ref}}\end{pmatrix} = \begin{pmatrix}0\\0\end{pmatrix}. \tag{4.4}$$

Although the solution was started with the parameters from the trimmed rigid model, in general the convergence was slow and approximately 20 iteration steps were necessary to obtain a trimmed flight state. Fig. 11 shows the reaction forces and moments during a trim iteration. It can be seen that all components are zero in the trimmed flight state.

Unlike with aircraft, not only the aerodynamic forces cause structural deflections. There are additional sources of nonlinearities which make the convergence slow. For example, due to the pressure gradient, the structural stiffness depends strongly on the pitch angle α. Nose-up leads to low internal pressure at the tail resulting in weak support for the

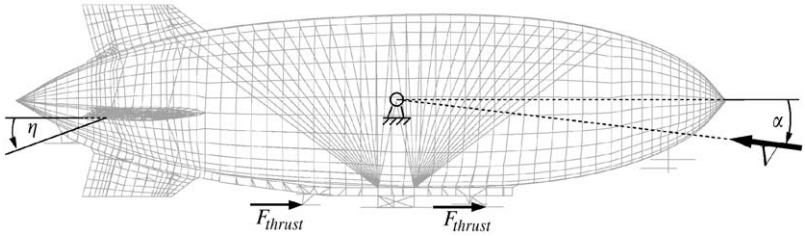

Fig. 9. Airship with degrees of freedom for the trimmed flight state.

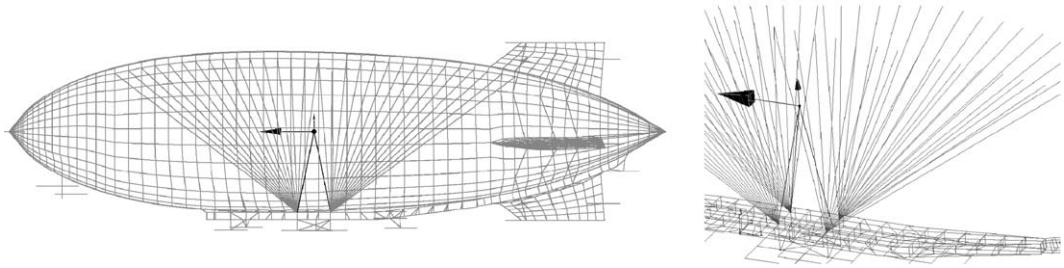

Fig. 10. Kinematic coupling of the load frame points (side view and inside view).

empennage, whereas nose-down has the opposite effect. Under real flight conditions the pressure changes by nearly 100% at the lower and upper fin connection (Fig. 12).

4.3. Inertia relief

Such structural models require the application of boundary conditions to eliminate the six rigid body degrees of freedom. In real free flight conditions these motions are allowed, and additional inertia effects had therefore to be taken into account—also for the static aeroelastic investigations performed.

The trimmed flight state is a reaction force and moment-free unaccelerated model state, to which several perturbations were additionally applied. The resulting manoeuvre flight state again features some structural reactions due to neglected acceleration fields for the airship. It is conceivable that the deformations and therefore the derivatives would differ in an accelerated state. The influence of the acceleration due to the motion and perturbations was investigated by applying accelerations obtained from the reaction forces and moments.

The accelerations were calculated assuming a linear elastic model. The reaction forces and the model mass yielded the translational accelerations

$$\mathbf{a} = \frac{\mathbf{RF}}{m}. \tag{4.5}$$

These, unlike the rotational accelerations, are independent of the reference point. The centre of mass c_M was chosen as the reference point, thus the reaction moments had first to be transferred to this point. The reaction moments were given with respect to the boundary condition point c_B and so the following transformation was used:

$$\mathbf{M}_M = \mathbf{RM}_B + (\mathbf{x}_M - \mathbf{x}_B) \times \mathbf{RF}_B. \tag{4.6}$$

The required rotational accelerations could then be calculated using the angular momentum balance for a rigid body around the centre of mass:

$$\boldsymbol{\Theta}_M \cdot \dot{\boldsymbol{\omega}}_M = \mathbf{M}_M. \tag{4.7}$$

By inverting the inertia tensor, this equation was solved for the rotational acceleration

$$\dot{\boldsymbol{\omega}}_M = \boldsymbol{\Theta}_M^{-1} \cdot \mathbf{M}_M. \tag{4.8}$$

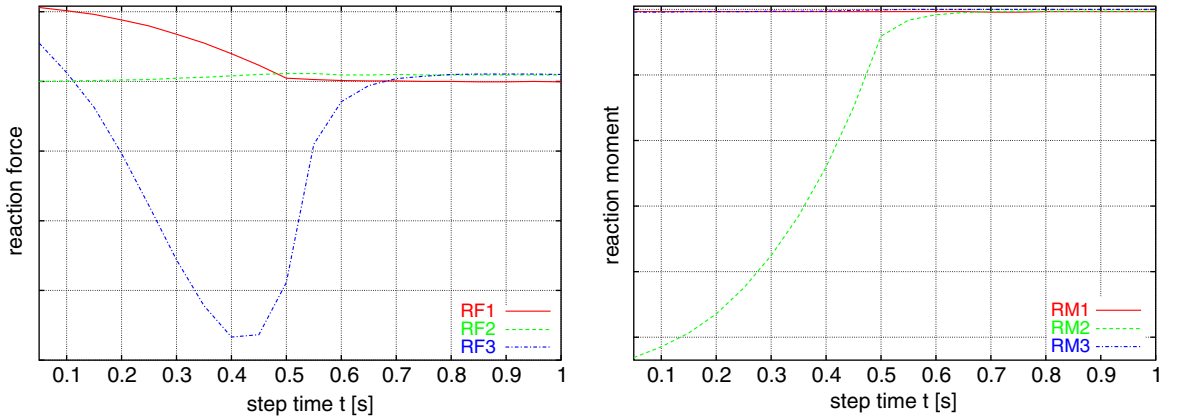

Fig. 11. Reaction forces and moments during a trim iteration.

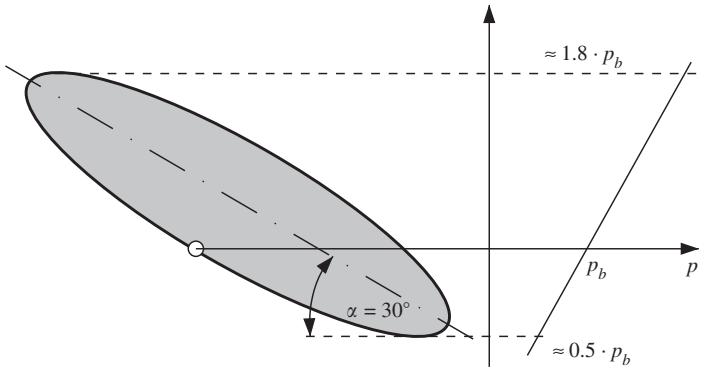

Fig. 12. Pressure distribution due to pitch angle.

The assumption of a linear model is the reason why the reaction forces and moments only vanish using iterative inertia relief. The iterative solution was obtained by two different nested iteration loops. The outer loop calculated the equilibrium for the investigated flight state coupled with fixed inertia corrections. The result of this calculation was a pressure distribution applied as a constant external load for the recalculation of the inertia correction. These new acceleration fields were applied again to a coupled (ABAQUS–VSAERO) calculation. This complex iterative procedure was continued until the residue became smaller than a reasonable tolerance.

The different inertia corrections had to be summed over each inertia correction run of n iterations by $\dot{\boldsymbol{\omega}} = \sum_{i=1}^{n} \dot{\boldsymbol{\omega}}_i$. In addition, the shifting of the centre of mass during the iterative process had to be taken into account. Its coordinates were averaged between two successive iterations.

The tolerance used for the residue was only applied to the reaction moments, as tests had shown that this results in forces being always minimised. The magnitude of the reaction moment vector must be lower than the predefined tolerance. A sensible tolerance was defined as a maximum shift in the centre of mass of length l_s (e.g. 0.1 m). Using a mass configuration of m_{Airship}, the residual resultant reaction moment was allowed to be $\Delta\mathbf{M}_B = m_{\text{Airship}} g l_s$. The convergence to a reaction force and moment-free, yet accelerated manoeuvre flight state is shown in Fig. 13.

4.4. Aeroelastic results and derivatives

To get an overview of the influence of the elastic deformation, the lift was calculated for different models and pitch angles. Five different structural models were compared:

`Rigid Model`: The rigid aerodynamic model (CAD geometry) with no deformation at all.

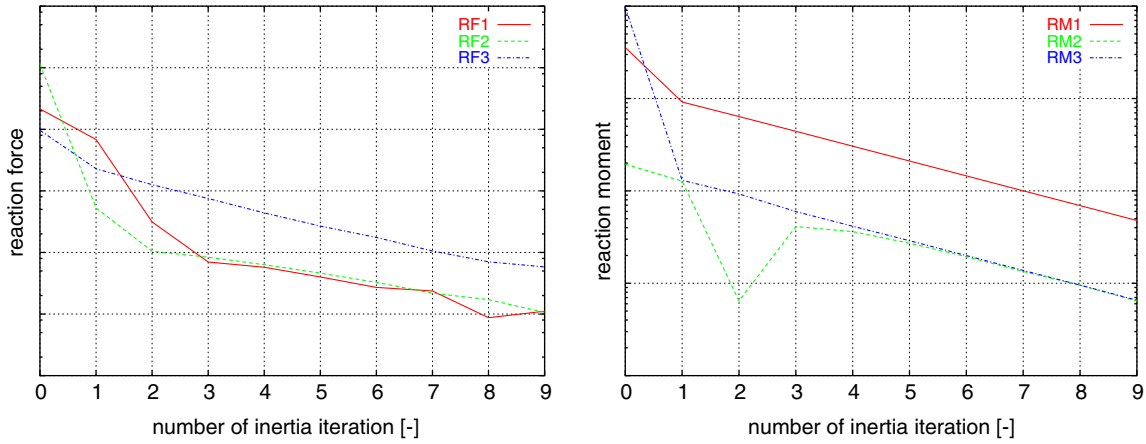

Fig. 13. Reaction forces and moments during an inertia relief analysis.

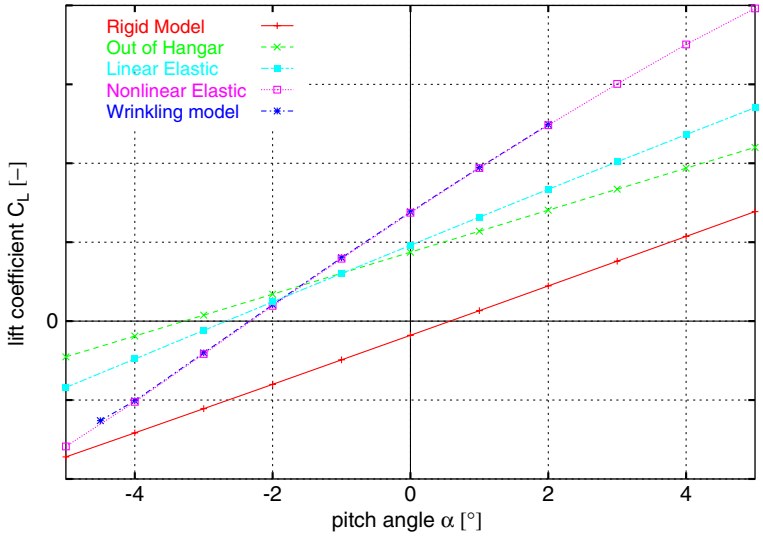

Fig. 14. Lift coefficient cL as a function of pitch angle α.

Out of Hangar: The assembled model deformed by the aerostatic loads and the gravity loads, remaining rigid during the aeroelastic calculation.

Linear Elastic: Linear elastic calculation for the out-of-hangar model.

Nonlinear Elastic: Nonlinear elastic calculation (out-of-hangar model), where the membrane can carry in-plane pressure.

Wrinkling Model: Nonlinear elastic calculation with a wrinkling model (membrane can not carry any in-plane pressure loads), Roddeman (1988).

Fig. 14 shows the different solutions compared by the lift coefficient characteristics $C_L(\alpha)$. It can easily be seen that different physical material models for the membrane have no influence on the aerodynamic coefficients—the "Nonlinear Elastic" and the "Wrinkling Model" models lead to the same results. Because no global wrinkling occurred for the applied flight conditions, it was not necessary to use the more time consuming wrinkling material model for the aeroelasticity calculations.

The rigid models "Rigid Model" and "Out of Hangar" show different C_L values, but the resulting derivatives $C_{L\alpha}$ (gradient, of C_L with respect to α) are very similar. Nevertheless, the difference of the shape between the two models revealed by the different pitch angles for zero lift shows the significance of the simulated assembly procedure leading to a deformed airship. Assuming linear elastic behaviour ("Linear Elastic"), the derivative rises compared to the rigid

models. In particular, a further increase was found when nonlinear elastic membrane behaviour was taken into account. This aspect leads to an increased zero lift angle of approximately 0.5° due to further deformations. The comparison of different models shows a significant influence of the structural nonlinearities on the derivatives.

In order to develop a meaningful model of the airship, it was necessary to make some assumptions which constrain the problem to practical bounds and which helps to provide dynamic visibility by reducing the equations of motion to a reasonably simple level. The assumptions according to Khoury and Gillett (1999) were: steady low-speed rectilinear flight; a stationary atmosphere; motion is described as a perturbation, not necessarily small, about an initial trimmed flight state; the mass of the airship remained constant; only rigid body motion was considered, the aeroelastic effects were included by the iterative procedure; the airship was symmetric about the x–z plane and the centres of buoyancy and gravity were in this plane; classical layout of the airship. Trim terms, which sum to zero, are removed from the linearised equation of motions, in addition to products and squares of small perturbation variables.

The longitudinal and lateral motions were investigated separately, through the assumption of equilibrium in the respective opposite direction. The trimmed flight state was disturbed by small perturbations in the degree of freedom being investigated. If the perturbations are small enough, a linearisation around the equilibrium state is allowed and the derivatives could be calculated by a differential quotient. Because the lateral controllability and stability are known to be more critical than those for the longitudinal direction, investigations were started using the lateral direction. The computation of the longitudinal derivatives was also realised with the described procedure.

The linearised lateral equations of motion describing small perturbation motion around the trimmed state are written in state space form:

$$M\dot{\mathbf{x}} = A\mathbf{x} + B\mathbf{u}, \tag{4.9}$$

where for lateral motion the state variables $\mathbf{x}^{\mathrm{T}} = \{v\ p\ r\ \phi\}$ are the perturbations for the side velocity v, for the roll rate p, for the yaw rate r and the roll angle ϕ. The only control variable $\mathbf{u}^{\mathrm{T}} = \{\zeta\}$ is the rudder angle perturbation ζ. The stability derivatives are given by the matrix A and the controllability derivatives by the matrix B, which can be normalised by the inertia matrix M:

$$A = \begin{bmatrix} Y_v & Y_p & (Y_r - m_x V) & 0 \\ L_v & L_p & (L_r - mz_M V) & L_\phi \\ N_v & N_p & (N_r - mx_M V) & N_\phi \\ 0 & 1 & 0 & 0 \end{bmatrix}, \quad B = \begin{bmatrix} Y_\zeta \\ 0 \\ N_\zeta \\ 0 \end{bmatrix}. \tag{4.10}$$

The side force derivatives Y and the moment derivatives L and N had to be obtained using the aeroelastic coupling procedure for each perturbation separately. For the moment derivatives due to the roll angle perturbation ϕ, the analytical solutions $L_\phi = -mgz_M \cos(\theta_T)$ and $N_\phi = -mgx_M \cos(\theta_T)$ can be used, where θ_T is the pitch attitude of the trimmed flight state. The definition of the mass and inertia terms are obtained from Khoury and Gillett (1999) and will not be listed here.

The eigenvalues of the normalised matrix A are the stability roots. They are used to judge the stability of the lateral modes: yaw subsidence, side slip subsidence and roll oscillation. The respective mode is stable if the real part of the

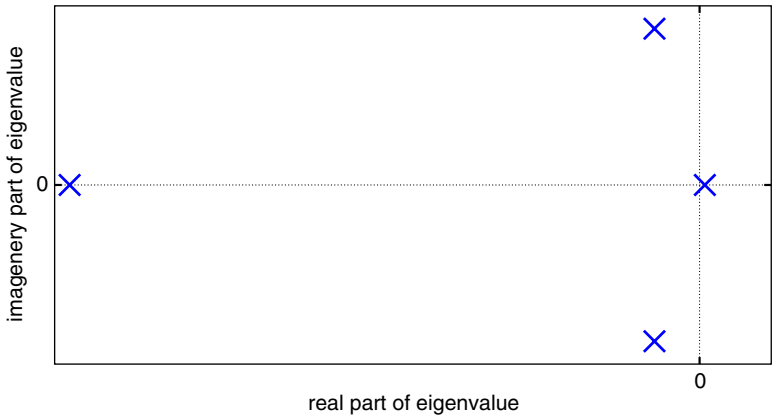

Fig. 15. Example of lateral stability roots.

complex eigenvalue is negative. The controllability of the airship in yaw is indicated by a negative third component of the normalised matrix B.

An example set of calculated lateral stability roots is plotted in Fig. 15. It was found that only the yaw subsidence mode is unstable for the investigated light airship with empty ballonets. This instability became smaller with each included additional physical phenomenon (e.g. flexibility, inertia effects).

5. Conclusion

In this work a method has been presented to investigate the nonlinear aeroelastic behaviour of an airship. The described procedure was developed and tested for the airship CL160, but is not limited to airships. It can also be used for other structures, especially for those with non-negligible elastic and nonlinear structural and/or aerodynamic behaviour (e.g. sails). To the authors' best knowledge, a comparable procedure has not been published, so the described technique can be considered to be unique. Unfortunately the investment in its development could not be capitalised upon due to the insolvency of CargoLifter.

The realised aeroelastic coupling method is able to handle all the nonlinearities present in the different models, and can deliver the required derivatives which would be difficult to obtain from free-flight or wind tunnel experiments. Nevertheless, the numerical results show very good agreement with some available internal experimental data. Using the suggested iterative coupling with integration of the described physical phenomena, all derivatives for stability and controllability investigations could be obtained. The example results presented for the lateral direction support this hypothesis. A final statement on the stability and controllability of the investigated configuration cannot be given because of the work being preliminary cut short.

In future work, a closer coupling between aerodynamics and structure would be made more efficient. Due to the iterative interchange of information, the proposed method is very time consuming. With regard to a transient flight model with the evaluation of the stability roots in each flight state defined by the time step, the fluid–structure interaction should be unified in a single code or carried out on parallel computer architectures. In the meantime, the influence of neglected aerodynamic surfaces, e.g. full keel, could be introduced by some calibrated scaling factors for the different components. The refinement of the discretisation could also be replaced by such correction factors obtained from the comparison of a full aerodynamic model and that used in the aeroelastic investigations.

Acknowledgements

The authors would like to express their particular gratitude to C. Potma of FlowMotion (The Netherlands) and to their former colleague E. d'Henin for the very informative discussions and the very helpful support provided on the investigations carried out.

The described procedure for the investigation of the aeroelastic properties was developed in the scope of the authors' daily work in the Flight Science department, CargoLifter Development GmbH.

References

Haas, R., Dietzius, A., 1913. Stoffdehnung und Formänderung der Hülle von Prall-Luftschiffen. Luftfahrt und Wissenschaft. Springer, Berlin.

Hibbitt, Karlsson & Sorensen, Inc., 2001. ABAQUS/Standard User's Manual and ABAQUS/Theory Manual. Abacom, version 6.23.

Khoury, G.A., Gillett, J.D., 1999. Airship Technology. Cambridge University Press, Cambridge.

MSC.Patran, 2001. User's Manual. MSC.Software Corporation, Version 2001.

Nathman, D.J.K., 1999. VSAERO—A Computer Program for Calculating the Nonlinear Aerodynamic Characteristics of Arbitrary Configurations/Users' Manual. Analytical Methods, Inc., version 6.1.

Press, W.H., Teukolsky, S.A., Vetterling, W.T., Flannery, B.P., 1996. Numerical Recipes in Fortran90. Cambridge University Press, Cambridge.

Roddeman, D.G., 1988. Force transmission in wrinkled membranes, a numerical tool to study connective tissue structures. Ph.D. thesis, Technische Universität Eindhoven, The Netherlands.

Zienkiewicz, O.C., Taylor, R.L., 1991. The Finite Element Method. McGraw-Hill, New York.